

## MEIONITE: RIETVELD STRUCTURE-REFINEMENT, $^{29}\text{Si}$ MAS AND $^{27}\text{Al}$ SATRAS NMR SPECTROSCOPY, AND COMMENTS ON THE MARIALITE–MEIONITE SERIES

BARBARA L. SHERRIFF<sup>§</sup>

*Department of Geological Sciences, University of Manitoba, Winnipeg, Manitoba R3T 2N2, Canada*

ELENA V. SOKOLOVA AND YURII K. KABALOV

*Department of Crystallography, Faculty of Geology, Moscow State University, Moscow, 119899, Russia*

DAVID M. JENKINS

*Department of Geological Sciences and Environmental Studies, Binghamton University,  
Binghamton, New York, 13902-6000, U.S.A.*

GERALD KUNATH-FANDREI, STEFFEN GOETZ AND CHRISTIAN JÄGER

*Institut für Optik and Quantenelektronik, Friedrich-Schiller-Universität, Max-Wien Platz 1, D-07743 Jena, Germany*

JULIUS SCHNEIDER

*Institut für Kristallographie und Angewandte Mineralogie, Universität München, D-80333 München, Germany*

### ABSTRACT

Rietveld structure refinement,  $^{29}\text{Si}$  magic angle spinning (MAS) and  $^{27}\text{Al}$  satellite transition (SATRAS) NMR spectroscopic data are given for three natural samples of meionite and for synthetic end-member meionite. Trends in structural parameters and NMR spectra are discussed for the solid-solution series from marialite to meionite. The  $a$  cell dimension and  $^{27}\text{Al}$  SATRAS NMR spectra show a continuous change through the series, whereas the space group,  $c$  cell dimension and  $^{29}\text{Si}$  MAS NMR spectra show different trends for the three subseries,  $\text{Si}_{9,0-8,3}$ ,  $\text{Si}_{8,3-7,4}$  and  $\text{Si}_{7,4-6,0}$ . Over the interval  $\text{Si}_{9,0-8,3}$ , the space group is  $I4/m$ , the  $c$  cell dimension increases with Al content, and  $^{29}\text{Si}$  spectra show multiple well-resolved peaks; the anion site is occupied by  $\text{Cl}^-$ , and the  $T(1)$  site, by Si. Si–Al order between the  $T(2)$  and  $T(3)$  sites causes the space group for  $\text{Si}_{8,3-7,4}$  to be  $P4_2/n$  and the  $^{29}\text{Si}$  MAS NMR spectra to be dominated by Si(1) (3Si1Al) and Si(3) (1Si3Al) peaks. Here, there is a negative correlation between  $c$  cell dimension and Al content. Over the interval  $\text{Si}_{7,4-6,0}$ , the  $c$  cell parameter increases with Al content, the space group is  $I4/m$ , and multiple  $^{29}\text{Si}$  MAS NMR peaks become broad and poorly resolved.  $\text{Ca}^{2+}$  continues to replace monovalent cations in the  $M$  site, and Al enters both the  $T(1)$  and  $T(2)$  sites, producing Al–O–Al bonds. In the natural end-member meionite, however, the Al–Si order is found to be 3:1 for  $T(1)$  and 3:5 for  $T(2)$ .

*Keywords:* scapolite, meionite, Rietveld structure-refinement,  $^{29}\text{Si}$  MAS NMR spectroscopy,  $^{27}\text{Al}$  SATRAS spectroscopy.

### SOMMAIRE

Nous présentons les résultats d'affinements de la structure (méthode de Rietveld) de trois échantillons naturels de méionite et d'un échantillon synthétique ayant la composition idéale, ainsi que des données en résonance magnétique nucléaire (RMN) portant sur le  $^{29}\text{Si}$  (spin à l'angle magique, MAS) et les transitions satellites (SATRAS) de l'ion  $^{27}\text{Al}$ . Les tendances des paramètres structuraux et des spectres RMN sont évaluées pour la solution solide complète entre marialite et méionite. Le paramètre réticulaire  $a$  et les spectres RMN SATRAS de  $^{27}\text{Al}$  font preuve de changements progressifs le long de cette série, tandis que le groupe spatial, la dimension  $c$  et les spectres RMN MAS de  $^{29}\text{Si}$  définissent des tracés différents pour les trois sous-séries,  $\text{Si}_{9,0-8,3}$ ,  $\text{Si}_{8,3-7,4}$  et  $\text{Si}_{7,4-6,0}$ . Dans le cas de l'intervalle  $\text{Si}_{9,0-8,3}$ , le groupe spatial serait  $I4/m$ , le paramètre réticulaire  $c$  augmente avec la teneur en Al, et les spectres  $^{29}\text{Si}$  possèdent de multiples pics bien résolus; le site de l'anion contient le  $\text{Cl}^-$ , et le site  $T(1)$ , le Si. La mise en ordre de Si et de Al entre les sites  $T(2)$  et  $T(3)$  mène au groupe spatial  $P4_2/n$  sur l'intervalle  $\text{Si}_{8,3-7,4}$ , et les spectres RMN MAS de  $^{29}\text{Si}$  montrent la prédominance des pics pour Si(1) (3Si1Al) et Si(3) (1Si3Al). Dans ce cas, il y a une corrélation négative entre la

<sup>§</sup> E-mail address: bl\_sherriff@umanitoba.ca

dimension  $c$  et la teneur en Al. Sur l'intervalle  $\text{Si}_{7.4-6.0}$ , le paramètre  $c$  augmente avec la teneur en Al, le groupe spatial est  $I4/m$ , et les pics multiples  $^{29}\text{Si}$  des spectres RMN MAS deviennent flous et non résolus. Le  $\text{Ca}^{2+}$  continue de remplacer les cations monovalents au site  $M$ , et l'aluminium occupe à la fois les sites  $T(1)$  et  $T(2)$ , produisant ainsi des liaisons Al–O–Al. Dans le cas de la méionite pure naturelle, toutefois, la mise en ordre de Al et Si mène aux proportions 3:1 dans  $T(1)$  et 3:5 dans  $T(2)$ .

(Traduit par la Rédaction)

*Most-clés:* scapolite, méionite, affinement de la structure, méthode de Rietveld, spectres de résonance magnétique nucléaire  $^{29}\text{Si}$  (spin à l'angle magique), spectres  $^{27}\text{Al}$  des transitions satellites.

## INTRODUCTION

The relationship among cation order, chemical substitution and structural parameters of the scapolite group has been discussed extensively since the early work of Shaw (1960a, b). Over the past few years, we have undertaken a complete study of structural parameters, chemical compositional trends and atomic order of these minerals (Sokolova *et al.* 1996, Teertstra & Sherriff 1996, 1997, Sherriff *et al.* 1998). This is the third of a series of papers (Sokolova *et al.* 1996, Sherriff *et al.* 1998) using both Rietveld structure-refinement of X-ray powder-diffraction data and high-resolution solid-state nuclear magnetic resonance (NMR) spectroscopy to examine representative samples across the marialite–meionite series in terms of both short- and long-range order.

Correlations of  $M$  and  $A$  site occupancy and unit-cell parameters with Si content indicate three different trends across the marialite–meionite series, with changes in

trends at  $\text{Al}_{3.6}\text{Si}_{8.4}$  and  $\text{Al}_{4.7}\text{Si}_{7.3}$  (Zolotarev 1993, Teertstra & Sherriff 1996, 1997). In the first paper in this series, Sokolova *et al.* (1996) examined the marialitic compositions and found a linear trend in the cell parameters and in degree of cation order for samples with  $9.0 > \text{Si} > 8.4$  atoms per formula unit, *apfu*. They also found evidence of Al–O–Al bonds despite the low Al content of these samples of scapolite, contrary to Loewenstein (1954), but in agreement with the calculations of bond energy by Tossell (1993). In the second paper, the structure and degree of cation order of intermediate compositions of scapolite with  $8.4 > \text{Si} > 7.3$  *apfu* were investigated using the same approach (Sherriff *et al.* 1998). In this paper, we concentrate on the Ca-rich members of the series, with  $\text{Si} < 7.3$  *apfu*. This range of compositions, with Si/Al ratios near 1.5, is the most commonly encountered (Teertstra & Sherriff 1997). We also examine relationships and trends that we have been found throughout the series.

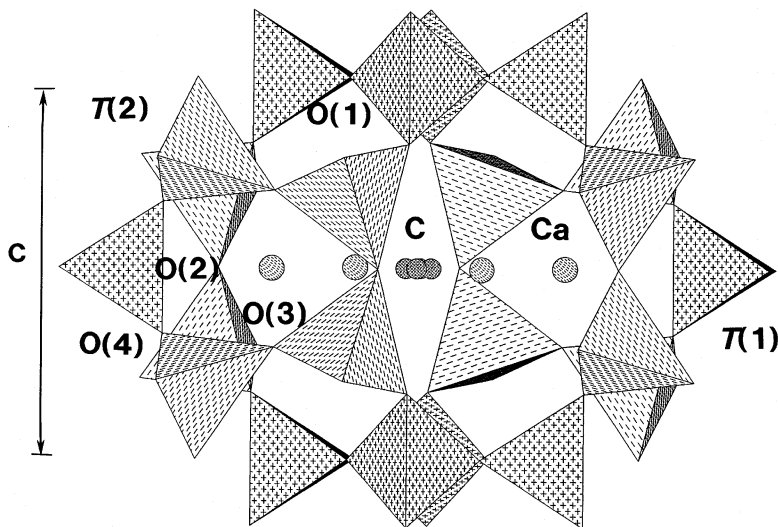


FIG. 1. A fragment of the crystal structure of meionite  $\text{Ca}_4\text{Al}_6\text{Si}_6\text{O}_{24}(\text{CO}_3)$  refined in space group  $I4/m$ , showing planar  $\text{Ca}_4\text{CO}_3$  group: crosses are  $T(1)\text{O}_4$  tetrahedra, and dashes,  $T(2)\text{O}_4$  tetrahedra.

## BACKGROUND INFORMATION

Scapolite-group minerals have a general formula  $M_4T_{12}O_{24}A$ , and constitute a solid-solution series between the idealized end-members  $Na_4Al_3Si_9O_{24}Cl$  (marialite, Ma) and  $Ca_4Al_6Si_6O_{24}CO_3$  (meionite, Me). The tetrahedral sites in scapolite form two types of four-membered rings, perpendicular to the  $c$  axis, one of them consisting of  $T(1)$  tetrahedra. In the space group  $I4/m$ , with a 4-fold rotation axis and an inversion center, the tetrahedra of the second type of four-membered ring are symmetrically equivalent, and are labeled  $T(2)$ . However, in the space group  $P4_2/n$ , rotation around the screw axis allows the separation of the  $T(2)$  sites into  $T(2)$  and  $T(3)$ . Viewed along the  $a$  axis, these rings join to form five-membered rings and define large cavities, each enclosing one  $A$ -anion surrounded by four alkali  $M$ -cations (Fig. 1). Scapolite-group minerals have three main forms of isomorphous substitution:  $Si^{4+}$  for  $Al^{3+}$  in the  $T$  site,  $Na^+$  for  $Ca^{2+}$  in the  $M$  site,  $Cl^-$  for  $CO_3^{2-}$  or  $SO_4^{2-}$  in the  $A$  site. There can also be minor amounts of K, Sr, Ba and Fe, but only trace quantities of Mg, Mn, Ti, P, Br and F have been measured (Teertstra & Sherriff 1997). Compositions of individual samples are here stated in terms of Si–Al occupancy of the  $T$  sites.

## EXPERIMENTAL PROCEDURES

*Materials*

BOLT is a transparent light violet scapolite from a marble pegmatite in Bolton, Massachusetts, U.S.A. Our sample contains traces of plagioclase and muscovite. SL–1 is a yellowish, opaque scapolite from the Slyudyanka mineral deposit, eastern Siberia, Russia. MONT is a colorless gem-quality scapolite from vugs in a marble block ejected from Monte Somma, Italy (Moecher 1988). Individual crystals from various vugs at Monte Somma have slightly different compositions, but our crystal of MONT is the closest natural sample to end-member meionite. It contains  $Si_{6.11}Al_{5.77}$ . ON7 is from Monmouth Township, Ontario, CA63A from Grand Calumet Township, Quebec, GL from Gib Lake, Ontario, Q26 from Clapham Township, Quebec, and Q13 from Huddersfield Township, Quebec. The electron-microprobe (EMP) compositions of this sample of MONT and of BOLT, ON7, CA63A, GL, Q26, and Q13 are given in Teertstra & Sherriff (1997).

Meionite (S.MEI) was synthesized from a mixture of reagent-grade CaO (decarbonated from  $CaCO_3$ ),  $Al_2O_3$ ,  $SiO_2$ , and  $CaCO_3$ , with the bulk composition  $3(CaAl_2Si_2O_8) \cdot 1.5(CaCO_3)$ . A slight excess in  $CaCO_3$  over the ideal composition of meionite  $[3(CaAl_2Si_2O_8) \cdot 1.0(CaCO_3)]$  ensures the presence of sufficient carbonate to saturate the system in  $CaCO_3$ . Any excess carbonate present after the synthesis was readily dissolved by treatment of the reaction products in dilute (10 wt%) HCl.

Syntheses were performed in a piston–cylinder press with a pressure chamber 12.7 mm in diameter using pressure media made from pressed  $SrCO_3$  powder, which has a higher thermal stability than the conventional NaCl pressure media. Portions of the oxide–carbonate starting mixture were loaded into crucibles made of ultra-pure graphite, dried at  $110^\circ C$  in air, and treated at  $1200 \pm 10^\circ C$  and  $14.5 \pm 0.5$  kbar for 48 hours. Temperatures were monitored with freshly prepared  $WRe_3$ – $WRe_{25}$  thermocouples. The resultant assemblage was in the form of a dense, finely crystalline aggregate, which was broken up and rinsed briefly (~1 min) in dilute HCl to remove any excess  $CaCO_3$ . X-ray characterization of the products of synthesis indicated a very high yield of meionite with only trace quantities of graphite, corundum, and possibly wollastonite present.

*Chemical analyses*

Chemical analyses of SL–1 and S.MEI were made with an electron microprobe (CAMECA SX–50) operating at 15 kV and 20 nA with a beam diameter of 10  $\mu m$  and count times of 20 s. The data reduction used the “PAP” procedure (Pouchou & Pichoir 1985). We used as principal reference standards gem-quality meionite from Brazil, U.S.N.M. #R6600–1 (Dunn *et al.* 1978), albite from the Rutherford mine, Amelia Courthouse, Virginia, anorthite from Sitkinak Island, Alaska, and tugtupite from the type locality in southern Greenland (R.O.M. #M32790). Compositions were determined on the same samples from which the X-ray data and NMR data were measured. The stoichiometric formulae for the five samples of scapolite were calculated using the method of Teertstra & Sherriff (1996, 1997) (Table 1).

*Rietveld structure-refinement*

X-ray powder-diffraction data of meionite BOLT, SL–1, and MONT were collected on an ADP–2 diffractometer using  $Cu K\alpha$  radiation (Ni filter), a step width of  $0.02^\circ 2\theta$  and a count time of 5 s per step. Powder-diffraction data for S.MEI were collected on a focusing STOE–STADIP diffractometer, equipped with a curved Ge (111) primary monochromator producing monochromatic  $MoK\alpha_1$  radiation ( $\lambda = 0.70926 \text{ \AA}$ ) with a minimum FWHM (full-width at half-maximum) of  $0.08^\circ$  according to the procedure described by Wölfel (1981). The sample was held in a quartz capillary, and rotated to minimize preferred orientation. Diffracted intensities were collected in a stepwise overlapping mode of a linear position-sensitive detector with about  $5^\circ$  acceptance angle and  $0.02^\circ$  channel (Wölfel 1983). Structure refinements were carried out with the Wyriet, version 3.3 program (Schneider 1989) in both space groups:  $I4/m$  and  $P4_2/n$ . The starting model was taken from Aitken *et al.* (1984) and Peterson *et al.* (1979), and ionic scattering factors were used. There was no evidence for lowering the symmetry, so we preferred

TABLE 1. CHEMICAL COMPOSITION OF MEIONITE

	BOLT*	SL-1	MONT*	S.MEI
SiO <sub>2</sub> wt%	46.01	43.67	39.31	37.95
Al <sub>2</sub> O <sub>3</sub>	27.07	28.73	31.50	31.93
TiO <sub>2</sub>	0.00	-	0.03	0.00
Fe <sub>2</sub> O <sub>3</sub>	0.04	0.08	0.11	0.01
Na <sub>2</sub> O	3.90	2.57	0.37	0.04
K <sub>2</sub> O	0.17	0.15	0.17	0.01
CaO	16.72	18.60	22.90	22.62
SrO	0.04	0.18	0.05	2.05
BaO	0.06	0.15	0.04	0.00
Cl	0.52	0.07	0.03	0.01
F	0.11	0.00	0.02	0.00
SO <sub>3</sub>	0.00	2.77	0.25	0.00
Sum	94.68	96.97	94.85	94.62
O=Cl,F	-0.16	-0.02	-0.01	0.00
Total	94.52	96.95	94.84	94.62
Si ( <i>apfu</i> )	7.09	6.79	6.11	6.03
Al	4.91	5.26	5.77	5.97
Fe <sup>3+</sup>	0.00	0.00	0.01	0.00
Na	1.17	0.77	0.11	0.01
K	0.21	0.03	0.03	0.00
Ca	2.76	3.10	3.82	3.85
Fe <sup>2+</sup>	0.00	0.01	0.00	0.00
Sr	0.00	-	0.00	0.03
Ba	0.00	-	0.00	0.00
Cl	0.14	0.02	0.01	0.00
F	0.05	0.00	0.01	0.00
S	0.00	0.32	0.03	0.00
C	0.88	0.66	0.91	1.02
Si/(Al+Fe <sup>3+</sup> )	1.44	1.29	1.06	1.01
%Me	69.8	79.5	96.3	99.7

The proportions of Fe<sup>3+</sup> and Fe<sup>2+</sup> were calculated as described in Teertstra & Sherriff (1996, 1997). \* Compositions from Teertstra & Sherriff (1997).

space group of *I4/m* for BOLT, SL-1, MONT and S.MEI. A Pearson profile function with 6 FWHM was used. Asymmetry was refined up to a 2 of 40°. The crystal structures of BOLT, SL-1, and S.MEI were refined in anisotropic approximation for cations and isotropic for anions, with 80 refined parameters. MONT was only refined with isotropic approximation and 41 refined parameters.

For the refinement of the *M*-site occupancy, K<sup>+</sup> was assigned according to the chemical composition determined and fixed, then the site occupancies for Na<sup>+</sup> (*Z* = 11) and Ca<sup>2+</sup> (*Z* = 20) were refined simultaneously. The scattering curve of Si<sup>4+</sup> was used for the refinement of the occupancies of the *T* sites. For all four samples of meionite, the crystal-structure model was supplemented by (CO<sub>3</sub>)<sup>2-</sup> anion adopting the coordinates from Aitken *et al.* (1984). For SL-1, which has 0.32 *S apfu*, the (SO<sub>4</sub>)<sup>2-</sup> anion was added according to coordinates taken from Peterson *et al.* (1979). Atomic coordinates, displacement parameters, and site occupancies for C, S and corresponding O atoms were fixed and not taken into the refinement. Thus, we present *M*-O(7-10) distances without estimated standard deviations. Tables of observed and calculated structure-factors are available from the Depository of Unpublished Data, CISTI, Na-

tional Research Council, Ottawa, Ontario K1A 0S2, Canada.

The <sup>29</sup>Si NMR spectra were recorded on the AMX500 spectrometer with a Doty magic angle spinning (MAS) probe at the Prairie Regional NMR Centre, Winnipeg, Manitoba, at a frequency of 99.36 MHz, with a recycle delay of 5 s, and referenced to <sup>29</sup>Si in tetramethylsilane (TMS). The number of Si atoms corresponding to each *T*-site environment was calculated from the relative intensities of the <sup>29</sup>Si peaks from computer simulations using a least-squares iterative process, which varied the isotropic chemical shift, the Gaussian and Lorentzian broadening parameters, and the intensity of each line. A range of recycle delays were explored for both <sup>29</sup>Si and <sup>27</sup>Al to ensure complete relaxation for the values chosen. The spectrum of S.MEI has a poor signal-to-noise ratio, despite being obtained with a 10-minute delay over a period of 3 days, owing to the lack of paramagnetic impurities, causing very slow relaxation. The simulation of S.MEI required a broad peak (probably due to Si in an amorphous form) to be included to duplicate the measured spectrum. This peak produced such a large error into the calculations of relative intensity that the results from S.MEI were excluded from calculations of cation order.

The <sup>27</sup>Al satellite transitions (SATRAS) NMR spectra were obtained on a Bruker AMX 400 spectrometer, at the Institut für Optik und Quantenelektronik, Friedrich-Schiller-Universität, Jena, Germany, at a frequency of 104.2 MHz. Rates of sample rotation of 14 kHz were obtained using a Bruker high-speed probe, spinning within an accuracy of ±3 Hz. A solid π-pulse of 8 μs was determined, and a 1 μs pulse was used for all samples, with a 0.2 s recycle delay. The baseline roll after phasing caused by the finite pulse-length and dead-time was corrected using the cubic spline fit in the spectrometer software. The spectra were referenced to an aqueous solution of AlCl<sub>3</sub>. Simulations of the satellite transitions, including a distribution of the quadrupole parameters (Kunath *et al.* 1992, Kunath-Fandrei *et al.* 1995), were performed on a Pentium processor using the theory of Skibsted *et al.* (1991). The results of simulations for MONT required extra peaks probably due to the impurities that caused the peak at -82 ppm in the <sup>29</sup>Si spectrum. As a result, the relative <sup>27</sup>Al intensities of the peak for MONT were not used in the calculations of cation order.

#### THE PROPERTIES OF CALCIC SCAPOLITE

The samples of Ca-rich scapolite have Si contents between 7.09 and 6.03 atoms per formula unit (Table 1), which places them between the inflections at Al<sub>4.7</sub>Si<sub>17.3</sub> (Teertstra & Sherriff 1997) and end-member meionite Al<sub>6</sub>Si<sub>6</sub>. Although the number of monovalent alkali cations decrease steadily toward the end-member meionite, the proportion of the monovalent anion, Cl<sup>-</sup>, is insignificant at all compositions except for BOLT (0.14

TABLE 2. MISCELLANEOUS REFINEMENT DATA FOR MEIONITE

	<i>a</i> (Å)	<i>c</i> (Å)	<i>V</i> (Å <sup>3</sup> )	Sp.gr.	2θ-range (°)	Refl.	<i>R<sub>p</sub></i>	<i>R<sub>wp</sub></i>	<i>R<sub>B</sub></i>	<i>R<sub>F</sub></i>	<i>s</i> *	<i>DWD</i> **	<i>σ<sub>x</sub></i> ***
BOLT	12.1476(1)	7.5636(1)	1116.11(1)	<i>I4/m</i>	12.00-150.00	1240	4.65	6.04	3.56	4.93	1.16	1.60	1.482
SL-1	12.1637(1)	7.5739(1)	1120.60(1)	<i>I4/m</i>	12.00-130.00	1026	4.55	5.98	3.60	4.83	1.17	1.55	1.530
MONT	12.1969(4)	7.5763(2)	1127.08(6)	<i>I4/m</i>	12.00-152.82	1276	5.96	7.68	4.31	4.44	1.73	0.81	2.240
S.MEI	12.2119(1)	7.5811(1)	1130.57(1)	<i>I4/m</i>	3.00-39.98****	290	2.46	3.16	1.83	2.17	1.00	0.91	1.570

*s* = *R<sub>wp</sub>*/*R<sub>exp</sub>*, *R<sub>exp</sub>* – expected value of *R<sub>wp</sub>*

\*\**DWD* = Durbin-Watson *d* statistic (Hill & Flack, 1987)

\*\*\**σ<sub>x</sub>* = multiplication factor for all e.s.d's according to (Bérar & Lelann, 1991)

\*\*\*\**λMoK<sub>α1</sub>*, for all the rest - *λCuK<sub>(α1+α2)</sub>*

*apfu*). Teertstra & Sherriff (1997) found that the anion substitution is disconnected from the alkali anion substitution and also from substitution involving the framework of tetrahedra, in the meionitic as in marialitic compositions of scapolite. SL-1 has a relatively high concentration of  $\text{SO}_4^{2-}$  at 0.32 *apfu*, but this is below the 0.5 *S apfu* required to characterize the mineral as silvalite (Teertstra *et al.* 1999). The refinement results and final atomic parameters for the calcic scapolites are given in Tables 2 and 3, and selected interatomic distances and angles, in Table 4.

The chemical shift and relative intensities for the <sup>29</sup>Si MAS NMR spectra of calcic scapolites (Fig. 2) were calculated from simulated spectra (Table 5). The peaks at -91 ppm and -106 ppm are assigned to *T*(2) (1Si3Al) and *T*(1) (3Si1Al) sites in accordance with the interpretations of Sherriff *et al.* (1987). The peaks between these two resonances could be due to either *T*(2) sites with fewer Al neighboring atoms, as in the sodic scapolites (Sokolova *et al.* 1996), or to *T*(1) sites with more Al replacing Si in adjacent *T* sites. As the latter situation is more probable, the peaks are allocated to *T*(1) sites with (2Si2Al) and (1Si3Al) neighbors at -100 and -95 ppm, respectively. The values of relative intensities of the peaks due to *T*(1) (1Si3Al), *T*(2) (1Si3Al) and *T*(2) (4Al) are less reliable than those due to *T*(1) (3Si1Al) and *T*(1) (2Si2Al) owing to the complete overlap between the peaks at -94, -91 and -88 ppm. The small peak at -82 ppm in the spectrum of MONT is probably due to impurities of Al-rich minerals.

With decreasing Si content, the intensity of the peak at -106 ppm decreases as Al enters the *T*(1) site, not only replacing Si but also decreasing the number of Si neighbors. There is a gradual trend of the <sup>29</sup>Si peaks to increase in frequency with Al content, *e.g.*, the *T*(1) (3Si1Al) peak increases from -106.3 ppm for BOLT to -105.0 ppm for S. MEI owing to the increasing number of Al atoms in the second sphere of cations (Sherriff *et al.* 1998).

The broad peak attributed to *T*(1) (2Si2Al) at about -100 ppm can be simulated by two or more peaks. These peaks could be due to adjacent cations being  $\text{Ca}^{2+}$ ,  $\text{Na}^+$ , or  $\text{K}^+$  or to adjacent anions being  $\text{Cl}^-$ ,  $\text{CO}_3^{2-}$ , or  $\text{SO}_4^{2-}$ , but

in either of these cases the relative intensity of the peak due to adjacent  $\text{Na}^+$  or  $\text{Cl}^-$  should approach zero in the spectra of samples MONT and S.MEI. As this is not the case, the 1.5 ppm difference in chemical shift is interpreted as being due to the adjacent Al atoms occupying either *T*(1) or *T*(2) sites. Sherriff *et al.* (1991) showed

TABLE 3. ATOMIC COORDINATES AND DISPLACEMENT FACTORS (Å<sup>2</sup>) OF MEIONITE IN SPACE GROUP *I4/m*

		BOLT	SL-1	MONT	S.MEI
<i>M</i>	<i>x</i>	0.3589(3)	0.3577(5)	0.3570(5)	0.3556(6)
	<i>y</i>	0.2843(5)	0.2838(7)	0.2820(7)	0.2798(6)
	<i>z</i>	0.5	0.5	0.5	0.5
	<i>B<sub>iso</sub></i>	2.27(8)	1.89(9)	1.7(1)	1.5(1)
<i>T</i> (1)	<i>x</i>	0.3403(5)	0.3409(5)	0.3409(7)	0.341(1)
	<i>y</i>	0.4099(5)	0.4096(5)	0.4083(7)	0.407(1)
	<i>z</i>	0	0	0	0
	<i>B<sub>iso</sub></i>	1.43(8)	1.7(1)	1.1(2)	2.2(1)
<i>T</i> (2)	<i>x</i>	0.6592(3)	0.6581(3)	0.6588(7)	0.6595(6)
	<i>y</i>	0.9132(3)	0.9133(3)	0.9143(5)	0.9136(6)
	<i>z</i>	0.7929(5)	0.7926(3)	0.7916(7)	0.7925(8)
	<i>B<sub>iso</sub></i>	1.53(5)	1.7(8)	1.3(1)	1.8(2)
<i>O</i> (1)	<i>x</i>	0.4580(8)	0.4588(9)	0.460(1)	0.461(1)
	<i>y</i>	0.3502(8)	0.3500(8)	0.349(1)	0.350(1)
	<i>z</i>	0	0	0	0
	<i>B<sub>iso</sub></i>	1.6(2)	1.7(3)	1.5(2)	1.9(5)
<i>O</i> (2)	<i>x</i>	0.6852(8)	0.6862(8)	0.683(1)	0.689(1)
	<i>y</i>	0.8744(8)	0.8756(8)	0.8771(9)	0.874(1)
	<i>z</i>	0	0	0	0
	<i>B<sub>iso</sub></i>	1.5(2)	1.5(2)	0.6(2)	2.4(5)
<i>O</i> (3)	<i>x</i>	0.3516(6)	0.3518(6)	0.3523(9)	0.351(1)
	<i>y</i>	0.9522(6)	0.9526(8)	0.9520(9)	0.948(1)
	<i>z</i>	0.7911(9)	0.7896(9)	0.792(1)	0.794(1)
	<i>B<sub>iso</sub></i>	2.0(1)	2.0(2)	1.3(2)	1.3(3)
<i>O</i> (4)	<i>x</i>	0.2693(6)	0.2680(8)	0.2683(9)	0.263(3)
	<i>y</i>	0.3685(5)	0.3657(6)	0.3676(7)	0.363(1)
	<i>z</i>	0.8239(9)	0.826(1)	0.822(2)	0.827(2)
	<i>B<sub>iso</sub></i>	2.0(2)	2.7(3)	1.2(2)	2.6(6)

Cl and S atoms were put in the site *A* (½,½,½), and C and O(7-10) were added to the structure model. C, O(7) - O(9) constitute a CO<sub>3</sub> triangle, S and O(10) form a SO<sub>4</sub> tetrahedron. For C, O(7), O(8), O(9), O(10), coordinates *x*, *y*, *z* and temperature factor *B<sub>iso</sub>* = 3.5 Å<sup>2</sup> were fixed. Atomic coordinates for C, O(7), O(8), O(9), O(10) were taken from Aitken *et al.* (1984), and for O(10), from Peterson *et al.* (1979).

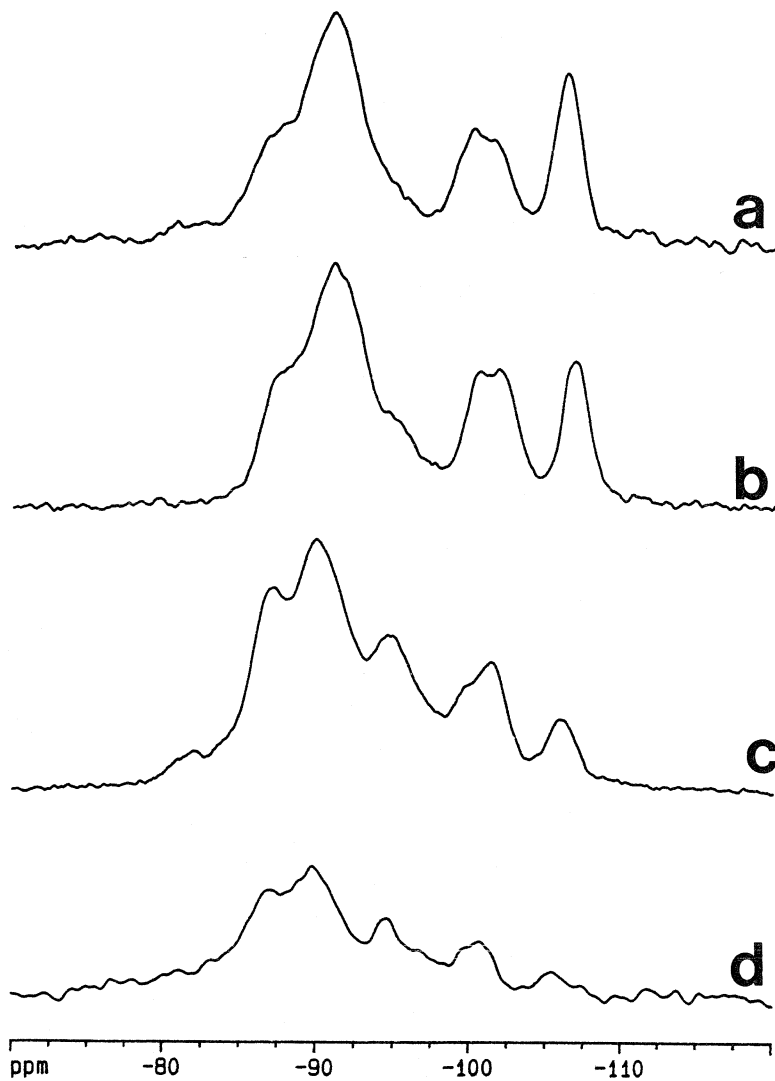


FIG. 2.  $^{29}\text{Si}$  MAS NMR spectra of (a) BOLD, (b) SL-1, (c) MONT, (d) S.MEI.

that the effect of the replacement of adjacent Si by Al on chemical shift increases with  $T\text{-O-T}$  angle. The average  $\langle T(1)\text{-O}(1)\text{-}T(1) \rangle$  angle is  $158.9^\circ$ , whereas the average  $\langle T(1)\text{-O}(4)\text{-}T(2) \rangle$  angle is  $137.6^\circ$ . Thus for the configuration Si(1) (2Si2Al), there are three possible combinations of Al: 2Al(1), Al(1)Al(2) and 2Al(2). The peak at  $-99.8$  ppm is assigned to Si(1)[2Si2Al(1)], and that at  $-101.5$  ppm, to Si(1)[2Si2Al(2)].

The number of Al-O-Al bonds per Al atom can be calculated from the relative intensities of the peaks fitted to each  $^{29}\text{Si}$  spectrum by using the formula:

$$\text{Al-O-Al} = 4 - \left( \sum_{m=0}^4 m I_{4,m} / \text{Al} \right) \quad (1)$$

modified from Engelhardt & Michel (1987).  $I$  is the intensity of the  $^{29}\text{Si}$  peaks with  $m$  Al atoms in the first coordination shell of  $T$  atoms, and Al represents the number of Al atoms per unit cell. The number of Al-O-Al bonds increases with Al content, from 0.3 for BOLT and 0.5 for SL-1 to 0.9 for MONT. The arrangement of tetrahedrally coordinated atoms around the five-membered rings makes the avoidance of Al-O-Al bonds impossible where the ratio Si/Al is less than two.

TABLE 4. SELECTED INTERATOMIC DISTANCES (Å) AND ANGLES (°) IN MEIONITE

	BOLT	SL-1	MONT	S.MEI
<i>T</i> (1)-O(1)	1.603(7)	1.607(8)	1.622(8)	1.63(2)
O(1)'	1.609(7)	1.605(8)	1.608(8)	1.61(2)
O(4)x2	1.665(5)	1.673(6)	1.689(6)	1.70(1)
< <i>T</i> (1)-O>	1.636	1.640	1.652	1.66
O(1)- <i>T</i> (1)-O(1)'	112.6(4)	112.9(4)	112.9(4)	111.3(7)
O(1)- <i>T</i> (1)-O(4)x2	109.0(3)	109.2(3)	109.7(3)	111.6(5)
O(1)- <i>T</i> (1)-O(4)'	109.9(2)	110.8(3)	109.1(3)	110.6(5)
O(1)- <i>T</i> (1)-O(4)'	106.3(3)	103.6(3)	106.1(3)	100.6(5)
<O- <i>T</i> (1)-O>	109.5	109.4	109.4	109.4
<i>T</i> (2)-O(2)	1.666(3)	1.672(3)	1.668(3)	1.685(5)
O(3)	1.640(5)	1.636(7)	1.636(5)	1.692(9)
O(3)'	1.672(5)	1.662(6)	1.674(5)	1.656(9)
O(4)	1.692(5)	1.713(6)	1.687(5)	1.673(9)
< <i>T</i> (2)-O>	1.668	1.671	1.666	1.677
O(2)- <i>T</i> (2)-O(3)	107.7(3)	107.5(3)	106.4(3)	107.4(5)
O(2)- <i>T</i> (2)-O(3)'	112.6(3)	113.2(3)	112.2(3)	113.8(5)
O(2)- <i>T</i> (2)-O(4)	104.5(3)	104.0(3)	104.6(3)	103.9(5)
O(3)- <i>T</i> (2)-O(3)'	112.3(3)	112.6(3)	112.6(3)	113.6(4)
O(2)- <i>T</i> (2)-O(4)	112.2(2)	112.8(3)	113.8(3)	115.5(4)
O(2)- <i>T</i> (2)-O(4)'	107.3(3)	106.4(3)	107.1(3)	102.4(4)
<O- <i>T</i> (2)-O>	109.4	109.4	109.5	109.4
<i>M</i> -O(2)	2.377(7)	2.366(8)	2.422(6)	2.34(1)
O(3)x2	2.550(5)	2.567(6)	2.550(5)	2.506(9)
O(4)x2	2.869(5)	2.880(6)	2.864(5)	2.909(8)
O(4)' <i>x</i> 2	2.765(5)	2.715(6)	2.736(5)	2.617(9)
< <i>M</i> -O>	2.678	2.670	2.675	2.629
<i>M</i> - <i>A</i>	3.131	2.750	3.018	3.302
<i>T</i> (1)-O(1)- <i>T</i> (1)'	157.4(4)	157.1(4)	157.1(5)	158.7(8)
<i>T</i> (2)-O(2)- <i>T</i> (2)'	140.2(2)	140.0(2)	142.2(3)	138.0(4)
<i>T</i> (2)-O(3)- <i>T</i> (2)'	147.7(3)	147.8(3)	147.3(3)	145.6(5)
<i>T</i> (1)-O(4)- <i>T</i> (2)'	136.9(2)	136.0(3)	136.3(5)	136.1(5)
< <i>T</i> -O- <i>T</i> >	145.6	145.2	145.7	144.6

The <sup>27</sup>Al SATRANS NMR spectra of BOLD and MONT can be simulated with three peaks (Table 6). The isotropic chemical shifts of the first two peaks have been calculated to be 57.7 and 60.1 ppm (Sherriff *et al.* 1998). The third peak could not be simulated with sufficient accuracy to calculate the isotropic chemical shift; it is given as a peak position. The higher-frequency peaks have been allocated to Al in the *T*(2) site adjacent to Cl (57.7 ppm), or CO<sub>3</sub> (60.1 ppm) because the relative intensities of these peaks were found to be proportional to the respective composition of the anion site (Sherriff *et al.* 1998). The lower-frequency peak is allocated to Al in the *T*(1) site. The frequencies of the isotropic chemical shift of the two *T*(2) peaks decrease with increasing Al content (Table 6), in contrast to those of the <sup>29</sup>Si peaks, which increase with Al content (Table 5). As <sup>27</sup>Al chemical shifts have been shown to be dependent on site symmetry, this decrease may be due to the decrease in the angle at the bridging O(2), O(3) and O(4) atoms as Al replaces Si.

TABLE 5. <sup>29</sup>Si MAS NMR CHEMICAL SHIFT AND RELATIVE INTENSITIES OF PEAKS CALCULATED AS Si *apfu* IN MEIONITE

	BOLT	SL-1	MONT
*Si ( <i>apfu</i> )	7.09	6.79	6.11
<i>T</i> 1(3Si1Al)	-106.3 ppm 1.29 Si	-106.1 ppm 0.93 Si	-105.4 ppm 0.45 Si
<i>T</i> 1(2Si2Al(2))	-101.5 ppm 0.96 Si	-101.6 ppm 0.76 Si	-101.4 ppm 0.61 ppm
<i>T</i> 1(2Si2Al(1))	-99.8 ppm 0.48 Si	-99.8 ppm 0.65 Si	-99.5 ppm 0.36 ppm
<i>T</i> 1(1Si3Al)	-94.5 ppm 0.78 Si	-94.5 ppm 1.27 Si	-94.5 ppm 1.67 Si
Total <i>T</i> 1	3.51 Si	3.61 Si	3.09 Si
<i>T</i> 2(1Si 3Al)	-90.9 ppm 2.60 Si	-91.0 ppm 2.13 Si	-90.0 ppm 1.86 Si
<i>T</i> 2(4Al)	-86.8 ppm 0.96 Si	-86.7 ppm 1.06 Si	-86.6 ppm 1.16 Si
Total <i>T</i> 2	3.56 Si	3.19 Si	3.02 Si

\* from EMP analyses

## TRENDS ACROSS THE SCAPOLITE SERIES

### Space group

Fifteen structures across the scapolite series have been refined in both *I4/m* and *P4<sub>2</sub>/n* space groups (Sokolova *et al.* 1996, 2000, Sherriff *et al.* 1998). In space group *I4/m*, there is a mirror plane *m<sub>z</sub>*, and there is no difference between the adjacent *T*(2,3) sites, whereas in space group *P4<sub>2</sub>/n*, the *T*(1) tetrahedron has a symmetry of *I*, and *T*(2) and *T*(3) have different occupancies. The final *R* values for each composition showed no significant difference between the two space groups. The number of *h + k + l ≠ 2n* weak reflections violating a body-centered cell remains almost constant at 46% of the total number of reflections in space group *P4<sub>2</sub>/n* for the intermediate samples, TANZ, PAM-5, MAD and MIN. No visual reflections violating *I*-centering were observed in the X-ray powder patterns for any of the 15 structures.

The choice of space-group symmetry was decided by the values of the *T*(2,3) interatomic distances. In space group of *P4<sub>2</sub>/n*, *T*(2) and *T*(3) have different *T*-O lengths and Si/Al occupancy. Only four scapolite samples, PAM-5, TANZ, MAD, MIN reveal significantly different <*T*(2)-O> and <*T*(3)-O> distances, indicating Si and Al order between these sites and a space group of *P4<sub>2</sub>/n*. For the remaining eleven samples, <*T*(2)-O> and <*T*(3)-O> distances are equal within the standard deviations, indicating the preferential space-group to be *I4/m*. Comparing our choice of space groups with previous single-crystal data (Belokoneva *et*

TABLE 6.  $^{27}\text{Al}$  MAS NMR ISOTROPIC CHEMICAL SHIFT ( $\delta_{\text{iso}}$ ) AND PEAK INTENSITIES AS Al *apfu* FOR SCAPOLITE SAMPLES

Sample	*Al <i>apfu</i>	<i>T</i> (2)Cl	<i>T</i> (2)(CO <sub>3</sub> )	<i>T</i> (1)**
PAM-1	3.12	59.3 ppm (3.1 Al)		
PAM-2	3.22	59.3 ppm (3.2 Al)		
PAM-3	3.24	59.3 ppm (3.2 Al)		
PAM-4	3.61	59.1 ppm (2.7 Al)	61.8 ppm (0.9 Al)	
TANZ	3.8	58.7 ppm (2.6 Al)	61.4 ppm (1.2 Al)	
ON7	3.93	58.5 ppm (2.0 Al)	60.7 ppm (1.8 Al)	65.8 ppm (0.1 Al)
CA63A	3.99	58.4 ppm (1.9 Al)	60.6 ppm (1.9 Al)	65.8 ppm (0.2 Al)
GL	4.02	58.4 ppm (2.1 Al)	60.6 ppm (1.9 Al)	65.6 ppm (0.1 Al)
MAD	4.24	58.3 ppm (1.7 Al)	60.6 ppm (2.2 Al)	66.4 ppm (0.3 Al)
Q26	4.27	58.2 ppm (1.6 Al)	60.6 ppm (2.3 Al)	66.5 ppm (0.3 Al)
Q13	4.49	58.1 ppm (1.4 Al)	60.3 ppm (2.7 Al)	66.1 ppm (0.4 Al)
MIN	4.53	57.8 ppm (0.8 Al)	60.0 ppm (3.3 Al)	67.1 ppm (0.4 Al)
BOLT	4.91	57.8 ppm (0.6 Al)	60.1 ppm (3.7 Al)	66.6 ppm (0.6 Al)

\* from EMP analyses. \*\* peak position not chemical shift.

*al.* 1991, 1993, Comodi *et al.* 1990, Papike & Zoltai 1965, Lin & Burley 1973a, b, 1975, Levien & Papike 1976, Papike & Stephenson 1966, Peterson *et al.* 1979, Aitken *et al.* 1984, Ulbrich 1973a, b) shows an agreement in the range of Si<sub>8.3-7.4</sub>. In the regions of Si<sub>9.0-8.3</sub> and Si<sub>7.4-6.0</sub>, both space groups have been used for the refinement of single-crystal data. There are no single-crystal data for marialite with more than 8.71 Si *apfu* (Belokoneva *et al.* 1993).

#### Framework angles

For all samples of scapolite, the *T*(1) tetrahedra are more regular than the *T*(2,3). The O–*T*(1)–O angle varies by 6.6° from 106.3° to 112.9°, and the O–*T*(2,3)–O angle, by 12.6°, from 102.9° to 115.5°.

There are four *T*–O–*T* angles in the scapolite structure if it is refined in space group *I4/m* (Fig. 1, Table 4) and six in space group *P4<sub>2</sub>/n* (Sherriff *et al.* 1998). According to Liebau (1985), *T*–O–*T* angles of 139° in framework silicates characterize unstressed (stable) bonds, and 160°, stressed (unstable) chemical bonds. The most stressed bonds in the scapolite structure lie in the (001) plane within the *T*(1) four-membered rings, with average <*T*(1)–O(1)–*T*(1)> angles of 158.9° (157.1° to 161.8°). The bonds within the *T*(2,3) rings, also belonging to the same plane, are somewhat less stressed, with average <*T*(2,3)–O(3)–*T*(2,3)> angles of 148.3° (145.6° to 150.7°). The least stressed bonds are between the *T*(2,3) sites parallel to the *c* axis, with average *T*(2,3)–O(2)–*T*(2,3) angles of 140.0° (138° to 142°). The bonds between the *T*(1) and *T*(2,3) rings, which are oriented at an angle of 30° to the *c* axis, have the smallest *T*(1)–O(4)–*T*(2,3) angles, with an average

of 137.6° (136.1° to 140.3°). There is no significant difference between the angles at oxygen atoms adjacent to either *T*(2) or *T*(3) in space group *P4<sub>2</sub>/n*.

#### Occupancy of the tetrahedrally coordinated sites

Structure refinement of intermediate compositions of scapolite in the space group of *P4<sub>2</sub>/n* shows Al and Si to be ordered at either the *T*(2) or *T*(3) sites, with a maximum degree of order at a Si:Al ratio of 2 (Sherriff *et al.* 1998). With either more or less Al, increasing disorder among the *T*(2,3) sites results in the increase of symmetry, with the space group changing to *I4/m*, and in an increase of the number of distinct Si environments, as seen in the  $^{29}\text{Si}$  MAS NMR spectra at Si:Al ratios of 3, 2, and 1 (Fig. 3).

Information about Si–Al occupancy of the *T* sites in scapolite-group minerals has previously been obtained from *T*–O distances (Lin & Burley 1973a, b, 1975). High-resolution  $^{29}\text{Si}$  and  $^{27}\text{Al}$  NMR spectra provide independent information on these occupancies. Table 7 shows the variations in bond distances and angles with Si and Al content, together with the site occupancies calculated from  $^{29}\text{Si}$  and  $^{27}\text{Al}$  NMR spectroscopy for natural samples of scapolite-group minerals. The difference of only ±0.2 *apfu* between the number of Al or Si sites [4 *T*(1) and 8 *T*(2,3)] obtained from chemical analysis and the summation of site occupancies from NMR spectroscopy confirms the assignment of individual peaks in these complex and, in some cases, poorly resolved spectra.

The <*T*(1)–O> bond distances, deduced from Rietveld structure-refinements, remain constant at 1.61–1.62 Å until the concentration of Al becomes greater than 4.24 *apfu*, at which point it increases gradually to 1.65 Å in the end member MONT (Table 7). Thus the Rietveld structure-refinement indicates that Al does not occupy the *T*(1) site until the total Al content is greater than 4.24 *apfu*.  $^{29}\text{Si}$  MAS NMR spectroscopy shows a decrease to 3.8 *apfu* for the Si content of the *T*(1) site in the spectrum of MAD with 4.24 Al *apfu*. The  $^{27}\text{Al}$  Al peak at 66 ppm assigned to the *T*(1) site is visible in the SATRAS spectrum of ON7 (3.93 Al *apfu*) and CA63A (3.99 Al *apfu*) (Table 6), indicating that Al enters the *T*(1) site if the Al content is less than 4 Al *apfu*. The maximum Al content of the *T*(1) site for the natural sample of end-member meionite can be calculated from the  $^{29}\text{Si}$  spectrum of MONT to be 1.0 *apfu*; this is contrary to previous ideas of Al–Si order (Lin & Burley 1975, Sherriff *et al.* 1987), that the *T*(1) site of end-member meionite would have equal occupancy by Al and Si. The unequal distribution of Si and Al among the tetrahedral sites is corroborated by the <*T*(1)–O> distance for MONT, which is 0.2 Å less than the <*T*(2)–O> distance.

The mean *T*(2,3)–O distance increases from 1.66 Å for PAM–1 to 1.68 Å where the Al content reaches 3.89 *apfu* in PAM–5 (Table 7). The lack of further increase

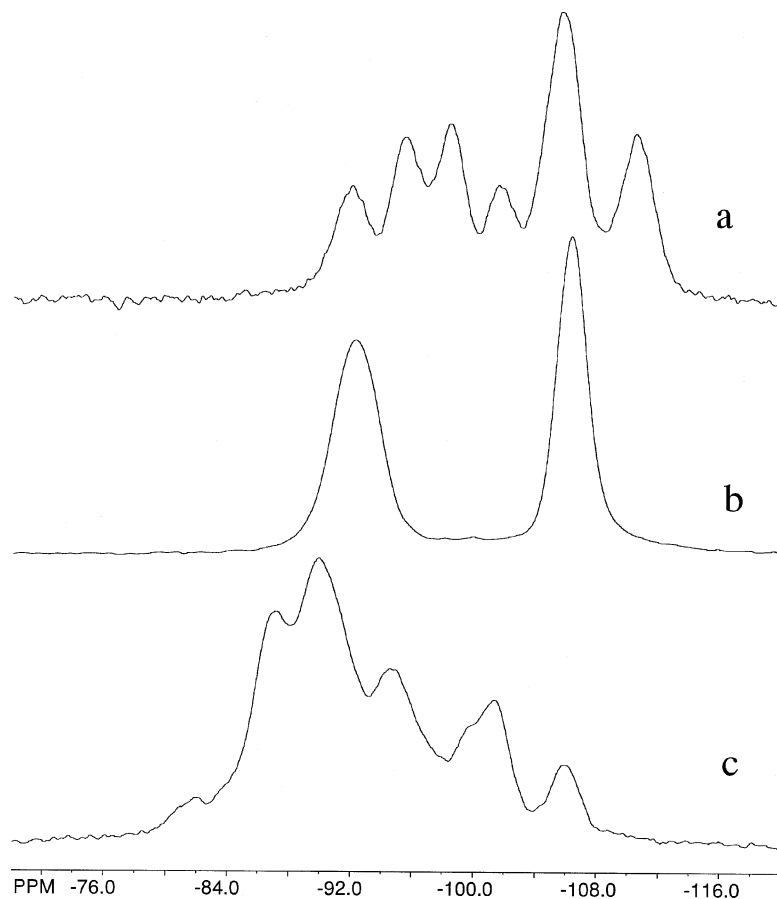


FIG. 3.  $^{29}\text{Si}$  MAS NMR spectra of (a) marialite PAM-1 (b) intermediate scapolite CA63A, (c) meionite MONT.

TABLE 7. *T* SITE OCCUPANCIES FROM NMR SPECTROSCOPY,  $\langle T\text{-O} \rangle$  BOND DISTANCES (Å) AND  $\langle T\text{-O-T} \rangle$  ANGLES ( $^\circ$ ) IN SCAPOLITE-GROUP MINERALS

	*Si <i>apfu</i>	*Al <i>apfu</i>	$\langle T(1)\text{-O} \rangle$	<i>T</i> (1) occupancy from NMR	$\langle T(2,3)\text{-O} \rangle$	<i>T</i> (2,3) occupancy from NMR	$\langle T(1)\text{-O}(1)\text{-T}(1) \rangle$	$\langle T(2)\text{-O}(2)\text{-T}(3) \rangle$	$\langle T(2,3)\text{-O}(3)\text{-T}(2,3) \rangle$	$\langle T(1)\text{-O}(4)\text{-T}(2,3) \rangle$
PAM-1	8.88	3.12	1.62 Å	4.0 Si, 0 Al	1.66 Å	4.9 Si, 3.1 Al	159.6 $^\circ$	139.2 $^\circ$	148.1 $^\circ$	136.9 $^\circ$
PAM-2	8.78	3.22	1.61 Å	4.0 Si, n.d.	1.66 Å	4.8 Si, n.d.	159.4 $^\circ$	141.4 $^\circ$	149.5 $^\circ$	140.3 $^\circ$
PAM-3	8.76	3.24	1.62 Å	4.0 Si, n.d.	1.65 Å	4.8 Si, n.d.	161.8 $^\circ$	141.3 $^\circ$	148.9 $^\circ$	138.4 $^\circ$
PAM-4	8.34	3.66	1.61 Å	4.0 Si, n.d.	1.66 Å	4.3 Si, n.d.	158.6 $^\circ$	140 $^\circ$	149 $^\circ$	137.4 $^\circ$
TANZ	8.16	3.83	1.61 Å	3.9 Si, 0 Al	1.67 Å	4.2 Si, 3.8 Al	158.5 $^\circ$	139 $^\circ$	149 $^\circ$	139 $^\circ$
PAM-5	8.11	3.89	1.61 Å	4.0 Si, n.d.	1.68 Å	4.1 Si, n.d.	160.8 $^\circ$	140 $^\circ$	148 $^\circ$	138 $^\circ$
MAD	7.76	4.24	1.62 Å	3.8 Si, 0.3 Al	1.68 Å	3.9 Si, 3.8 Al	159.6 $^\circ$	138 $^\circ$	149 $^\circ$	137 $^\circ$
MIN	7.47	4.53	1.63 Å	3.5 Si, 0.4 Al	1.68 Å	4.0 Si, 3.9 Al	158.3 $^\circ$	139 $^\circ$	147 $^\circ$	137 $^\circ$
BOLT	7.09	4.91	1.64 Å	3.5 Si, 0.6 Al	1.67 Å	3.6 Si, 4.3 Al	157.4 $^\circ$	140.2 $^\circ$	147.7 $^\circ$	136.9 $^\circ$
SL-1	6.79	5.26	1.64 Å	3.6 Si, n.d.	1.67 Å	3.2 Si, n.d.	157.1 $^\circ$	140 $^\circ$	147.8 $^\circ$	136 $^\circ$
MONT	6.11	5.77	1.65 Å	3.0 Si, n.d.	1.67 Å	3.1 Si, n.d.	157.1 $^\circ$	142.2 $^\circ$	147.3 $^\circ$	136.3 $^\circ$

n.d. = not determined. \* from electron-microprobe results.

with Al content indicates that the occupancy of the  $T(2,3)$  remains 4 Si and 4 Al. However, the relative intensities of the  $T(2,3)$   $^{29}\text{Si}$  MAS NMR peaks show a continuous decrease from 4.9 Si *apfu* for PAM-1 to 3.1 Si *apfu* for MONT. The  $^{27}\text{Al}$  SATRAS spectra also indicate a continuous increase in Al content (Table 6). Therefore, the NMR data indicate that the distribution of Si/Al in natural end-member meionite is closer to 3:1 in the  $T(1)$  site and 3:5 in the  $T(2,3)$  site than the 2:2 and 4:4 distribution previously postulated from bond distances. The Si/Al ratios for the  $T(1)$  and  $T(2,3)$  sites for marialite are confirmed to be 4:0 and 5:3, and for the intermediate scapolites, 4:0 and 4:4, respectively.

#### *M* and *A* sites

From S.MAR to S.MEI,  $\langle M-O \rangle$  decreases from 2.780 to 2.629 Å in accordance with increasing amount of  $\text{Ca}^{2+}$ , as the effective ionic radius for  $^{VIII}\text{Ca}^{2+}$  is 1.12 Å, and that for  $^{VIII}\text{Na}^{+}$  is 1.18 Å (Shannon 1976). The partial occupancy by  $\text{K}^{+}$  (1.51 Å) for some scapolites does not apparently affect the size of the *M* site. The longest *M*-ligand distance, from the *M* cation to the *A* site, varies from 2.860 to 3.131 Å. The maximum *M*-*A* distance of 3.302 Å was measured for S.MEI, in which  $\text{CO}_3$  is disordered across a center of symmetry and *A* actually is vacant. The *M*-ligand distances are much less sensitive to the chemical variations than the size of the *T* sites.

The refinement of  $\text{Ca}^{2+}$ ,  $\text{Na}^{+}$ , and  $\text{K}^{+}$  occupancies in the *M* site indicates the usual existence of vacancies, so that the composition can be presented as  $(\text{Ca}, \text{Na}, \text{K}, \square)$  (Table 8). In the Rietveld refinement procedure, alkali-site occupancies were initially assigned on the basis of electron-microprobe (EMP) results. Then, the K occupancy was fixed, and the site occupancies for the two cations  $\text{Ca}^{2+}$  ( $Z = 20$ ) and  $\text{Na}^{+}$  ( $Z = 11$ ) were refined. Although the Rietveld method usually underestimates site occupancies, the correlation between the results of EMP analyses and site refinement indicates the existence of up to 10% of vacancies in the *M* site. The disor-

dered distribution of the oxygen atoms of the  $\text{CO}_3^{2-}$  anion make confirmation of the vacancies inferred on the basis of *M*-O distances very problematic, but there does appear to be a relationship between  $\text{CO}_3^{2-}$  content and vacancies at the *M* site. There are no vacancies in marialite.

#### Cell parameters

Figure 4 presents plots of cell parameters *versus* Si *apfu* for the fifteen samples of scapolite investigated by Rietveld refinement from X-ray powder-diffraction data (Tables 1, 4; Sokolova *et al.* 1996, 2000, Sherriff *et al.* 1998). The cell parameters of marialite [ $a$  12.0396(2),  $c$  7.5427(2) Å] are smaller than the values predicted by Teertstra & Sherriff (1996) ( $a$  12.06,  $c$  7.551 Å), and those for meionite [ $a$  12.2119(1),  $c$  7.5811(1) Å] are greater than predicted ( $a$  12.20,  $c$  7.556 Å). This results in unit-cell volumes (*V*) that are the lowest and highest recorded for scapolite-group minerals.

As the increase in the *a* cell dimension from marialite to meionite is over four times that of the *c* cell dimension, the trends in *a* cell parameter are the predominant influence on the unit-cell volume *V* (Figs. 4a, c). In the range of  $9.00 > \text{Si} > 8.3$  *apfu*, *i.e.*, from S.MAR to PAM-4, there is an initial increase in *a* and *V* with Si *apfu*, but this is followed by a decrease in *a*. In the range  $8.3 > \text{Si} > 6.0$  *apfu*, the *a* and *V* parameters increase linearly with Al. These are the same trends in *a* and *V* found by Teertstra & Sherriff (1996). The more precise unit-cell dimensions from the Rietveld refinements of powder data have allowed us to delineate trends in *c* with decreasing Si content (Fig. 4b). The *c* parameter increases from 7.5427 to 7.5809 Å in the range of  $9.0 > \text{Si} > 8.3$  *apfu* (S.MAR to PAM-4), then decreases in the range of  $8.3 > \text{Si} > 7.4$  *apfu*. There is again an increase in *c* for  $7.09 > \text{Si} > 6.00$  *apfu*, but at a slower rate than for  $9.0 > \text{Si} > 8.3$  *apfu*. Zolotarev (1993) described similar correlations for *c versus* Si *apfu* based on powder data from the literature.

TABLE 8. OCCUPANCY OF *M* SITE BY ALKALI CATIONS IN SCAPOLITE-GROUP MINERALS

	PAM-1	PAM-2	PAM-3	S-1#	S-2#	PAM-4	TANZ	PAM-5	MAD	MIN	BOLT	SL-1	MONT
Na *	3.49	3.41	3.53	3.35	3.21	3.11	2.63	2.42	2.00	1.53	1.17	0.77	0.11
**	3.43	3.52	3.36	3.32	2.77	2.93	2.22	2.12	1.65	1.64	1.17	0.78	0.05
K *	0.28	0.27	0.17	0.24	0.11	0.05	0.25	0.20	0.10	0.14	0.21	0.03	0.03
**	0.25	0.26	0.19	0.24	0.13	0.00	0.25	0.20	0.10	0.14	0.20	0.01	0.02
Ca *	0.18	0.29	0.29	0.38	0.62	0.83	1.10	1.33	1.83	2.24	2.76	3.10	3.84
**	0.16	0.22	0.31	0.37	0.79	0.80	1.08	1.30	1.82	2.02	2.82	2.86	3.60
Fe <sup>2+</sup> *	0.01	0.01	0.00	0.01	0.01	0.00	0.01	0.00	0.01	0.00	0.00	0.01	0.00
□ *	0.04	0.02	0.01	0.02	0.05	0.01	0.01	0.05	0.06	0.09	-(0.14)	0.09	0.02
**	0.16	0.00	0.14	0.07	0.31	0.27	0.45	0.38	0.43	0.20	-(0.19)	0.35	0.33

\* from electron-microprobe results. \*\* from Rietveld structure refinement. # EMP data from Zolotarev (1993); the SREF results are from Sokolova *et al.* (2000).

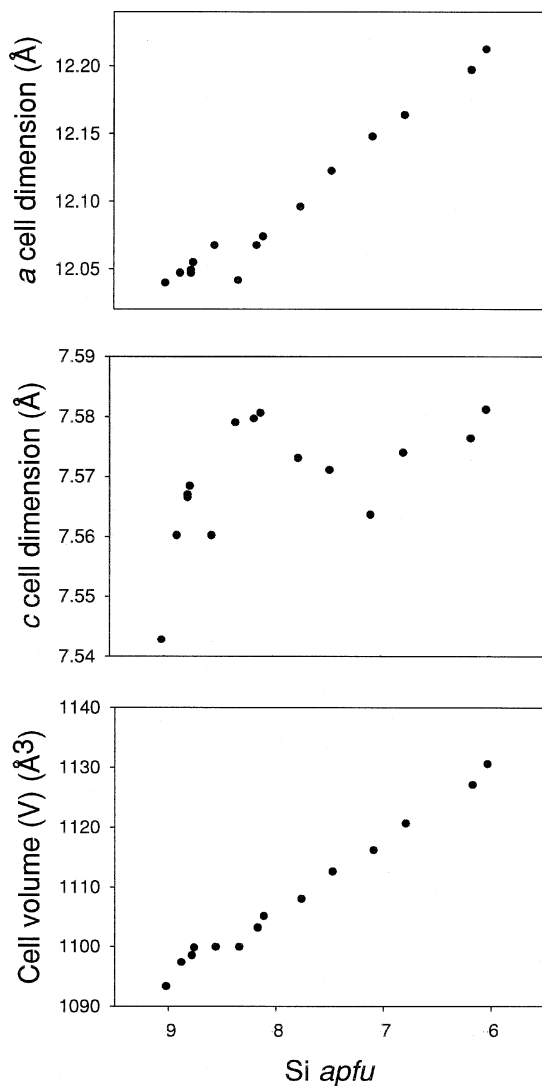


FIG. 4. The cell parameters  $a$ ,  $c$ , and  $V$  plotted against Si content. The structural and chemical data are taken from Tables 1 and 4 and also from Sokolova *et al.* (1996, 2000) and Sherriff *et al.* (1998).

Substitution involving the  $T$ ,  $M$ , and  $A$  sites provides an explanation for these variations in cell dimensions. The replacement of tetrahedrally coordinated  $\text{Si}^{4+}$  (effective ionic radius 0.26 Å) by  $\text{Al}^{3+}$  (effective ionic radius 0.39 Å) in either of the  $T$  sites could cause a maximum increase of 0.13 Å. The replacement of  $\text{Na}^+$  in eightfold coordination (effective ionic radius 1.18 Å) by  $\text{Ca}^{2+}$  (effective ionic radius 1.12 Å) in the  $M$  site leads to a decrease of 0.06 Å. Occupancy of the  $M$  site by  $\text{K}^+$  (effective ionic radius 1.51 Å) also needs to be consid-

ered. Substitution of  $\text{Cl}^-$  by a  $\text{CO}_3^{2-}$  group lying perpendicular to the  $c$  axis could cause a decrease in the  $c$  cell dimension of 0.46 Å and an increase in  $a$  of 0.91 Å.

The decrease in  $c$  and the increase in  $a$  cell dimensions with meionite content in the range  $8.3 > \text{Si} > 7.4$  apfu are most probably due to the effect of the planar  $\text{CO}_3^{2-}$  group replacing the relatively large and spherical  $\text{Cl}^-$  anion. At the meionite end of the series,  $7.4 > \text{Si} > 6.0$  apfu, the  $A$  site is totally occupied by  $\text{CO}_3^{2-}$ , and  $\text{Ca}^{2+}$  is substituting for  $\text{Na}^+$  in the  $M$  site, and Al, for Si in the  $T(1)$  and  $T(2,3)$  sites. The increase in both the  $a$  and  $c$  cell dimensions must be due to the Al-for-Si substitution.

## CONCLUSIONS

The three subseries characterized by distinct trends in atomic substitutions and order found by Zolotarev (1993) and Teertstra & Sherriff (1996, 1997) are confirmed by  $^{29}\text{Si}$  MAS NMR, changes in space groups, and trends in cell parameters.

The sodic scapolite subseries,  $9.0 > \text{Si} > 8.3$  apfu, is characterized by the space group  $I4/m$ , multiple well-resolved peaks in the  $^{29}\text{Si}$  spectra, and  $c$  cell dimensions that increase with Al content. In these compositions, the  $A$  site is totally occupied by  $\text{Cl}^-$ , and the  $T(1)$  sites, by Si,  $\text{Ca}^{2+}$  substitutes for  $\text{Na}^+$  in the  $M$  site, and Al increases in the  $T(2)$  site.

Ordering of Si and Al between the  $T(2)$  and  $T(3)$  sites causes the space group for the intermediate scapolites,  $8.3 > \text{Si} > 7.4$  apfu, to be  $P4_2/n$ . In these ordered compositions, the  $^{29}\text{Si}$  MAS NMR spectra are dominated by peaks due to Si(1) (3Si1Al) and Si(3) (1Si3Al), and there is a negative correlation between the  $c$  cell dimension and Al content. In this subseries, as Al replaces Si in both the  $T(1)$  and  $T(2)$  sites with no Al–O–Al bonds,  $\text{CO}_3^{2-}$  substitutes for  $\text{Cl}^-$  in the  $A$  site, and divalent  $\text{Ca}^{2+}$  plus vacancies substitute for monovalent  $\text{Na}^+$  and  $\text{K}^+$  in the  $M$  site.

In the calcic subseries,  $7.4 > \text{Si} > 6.0$  apfu, the  $c$  cell parameter increases with Al content, the space group is again  $I4/m$ , and the multiple  $^{29}\text{Si}$  MAS NMR peaks become broad and poorly resolved. In these compositions, the anion site is almost totally occupied by  $\text{CO}_3^{2-}$ ,  $\text{Ca}^{2+}$  continues to replace monovalent cations in the  $M$  site, and Al continues to enter both the  $T(1)$  and  $T(2)$  sites, giving Al–O–Al bonds. However, the Al/Si order in natural end-member meionite is found to be 3:1 for  $T(1)$  and 3:5 for  $T(2)$ , not 2:2 and 4:4 as previously proposed.

## ACKNOWLEDGEMENTS

Samples were kindly provided by D. Moecher and A.P. Khomyakov. This work was supported by Russian Fund for Basic Research, grant N00–05–65399 to EVS and YuKK, a NATO award to BLS and EVS, and a Natural Sciences and Engineering Research Council University Research Fellowship and Research Grant to

BLS. Our thanks go to two anonymous reviewers and to Dr. R.F. Martin for constructive comments on this manuscript.

## REFERENCES

- AITKEN, B.G., EVANS, H.T., JR. & KONNERT, J.A. (1984): The crystal structure of a synthetic meionite. *Neues Jahrb. Mineral., Abh.* **149**, 309-324.
- BELOKONEVA, E.L., SOKOLOVA, N.V. & DOROKHOVA, G.I. (1991): Crystal structure of natural Na,Ca-scapolite – an intermediate member of the marialite–meionite series. *Sov. Phys. Crystallogr.* **36**, 828-830.
- \_\_\_\_\_, \_\_\_\_\_ & URUSOV, V.S. (1993): Scapolites – crystalline structures of marialite (Me 11) and meionite (Me 88) – spatial group as a function of composition. *Kristallografiya* **38**, 52-57 (in Russ.).
- BÉRAR, J.-F. & LELANN, P. (1991): E.S.D's and estimated probable error obtained in Rietveld refinements with local correlations. *J. Appl. Crystallogr.* **24**, 1-5.
- COMODI, P., MELLINI, M. & ZANAZZI, P.F. (1990): Scapolites: variation of structure with pressure and possible role in the storage of fluids. *Eur. J. Mineral.* **2**, 195-202.
- DUNN, P.J., NELEN, J.E. & NORBERG, J. (1978): On the composition of gem scapolites. *J. Gemmol.* **16**, 4-10.
- ENGELHARDT, G. & MICHEL, D. (1987): *High Resolution Solid State NMR of Silicates and Zeolites*. John Wiley and Sons, New York, N.Y.
- HILL, R.G. & FLACK, H.D. (1987): The use of the Durbin–Watson *d* statistic in Rietveld analysis. *J. Appl. Crystallogr.* **20**, 356-361.
- KUNATH, G., LOSSO, P., STEUERNAGEL, S., SCHNEIDER, H. & JÄGER, C. (1992): <sup>27</sup>Al satellite transition spectroscopy (SATRAS) of polycrystalline aluminium borate 9Al<sub>2</sub>O<sub>3</sub>•2B<sub>2</sub>O<sub>3</sub>. *Solid State Nuclear Magn. Res.* **1**, 261-266.
- KUNATH-FANDREI, G., BASTOW, T.J., HALL, J.S., JÄGER, C. & SMITH, M.E. (1995): Quantification of aluminum coordination in amorphous alumina by combined central and satellite transition magic-angle spinning NMR. *J. Phys. Chem.* **99**, 15138-15141.
- LEVIEN, L. & PAPIKE, J.J. (1976): Scapolite crystal chemistry: aluminum-silicon distributions, carbonate group disorder and thermal expansion. *Am. Mineral.* **61**, 864-877.
- LIEBAU, F. (1985): *Structural Chemistry of Silicates. Structure, Bonding, and Classification*. Springer-Verlag, Berlin, Germany.
- LIN, S.B. & BURLEY, B.J. (1973a): Crystal structure of a sodium and chlorine-rich scapolite. *Acta Crystallogr.* **B29**, 1272-1278.
- \_\_\_\_\_, \_\_\_\_\_ & \_\_\_\_\_ (1973b): The crystal structure of meionite. *Acta Crystallogr.* **B29**, 2024-2026.
- \_\_\_\_\_, \_\_\_\_\_ & \_\_\_\_\_ (1975): The crystal structure of an intermediate scapolite – wernerite. *Acta Crystallogr.* **B31**, 1806-1814.
- LOEWENSTEIN, W. (1954): The distribution of aluminum in the tetrahedra of silicates and aluminates. *Am. Mineral.* **39**, 92-96.
- MOECHEER, D.P. (1988): *Scapolite Phase Equilibria and Carbon Isotope Variations in High Grade Rocks: Tests of the CO<sub>2</sub>-Flooding Hypothesis of Granulite Gneiss*. Ph.D. thesis, Univ. of Michigan, Ann Arbor, Michigan.
- PAPIKE, J.J. & STEPHENSON, N.C. (1966): The crystal structure of mizzonite, a calcium- and carbonate-rich scapolite. *Am. Mineral.* **51**, 1014-1027.
- \_\_\_\_\_, \_\_\_\_\_ & ZOLTAI, T. (1965): The crystal structure of a marialite scapolite. *Am. Mineral.* **50**, 641-655.
- PETERSON, R.C., DONNAY, G. & LEPAGE, Y. (1979): Sulfate disorder in scapolite. *Can. Mineral.* **17**, 53-61.
- POUCHOU, J.-L. & PICHOR, F. (1985) "PAP" (phi-rho-Z) procedure for improved quantitative microanalysis. In *Microbeam Analysis* (J.T. Armstrong, ed.). San Francisco Press, San Francisco, California (104-106).
- SCHNEIDER, J. (1989): Profile refinement on IBM-PC's. IUCr Int. Workshop on the Rietveld Method (Petten), 71 (abstr.).
- SHANNON, R.D. (1976): Revised effective ionic radii and systematic studies of interatomic distances in halides and chalcogenides. *Acta Crystallogr.* **A32**, 751-767.
- SHAW, D.M. (1960a): The geochemistry of scapolite. I. Previous work and general mineralogy. *J. Petrol.* **1**, 218-260.
- \_\_\_\_\_, \_\_\_\_\_ (1960b): The geochemistry of scapolite. II. Trace elements, petrology, and general geochemistry. *J. Petrol.* **1**, 261-285.
- SHERRIFF, B.L., GRUNDY, H.D. & HARTMAN, J.S. (1987): Occupancy of *T* sites in the scapolite series: a multinuclear NMR study using magic-angle spinning. *Can. Mineral.* **25**, 717-730.
- \_\_\_\_\_, \_\_\_\_\_ & \_\_\_\_\_ (1991): The relationship between <sup>29</sup>Si MAS NMR chemical shift and silicate mineral structure. *Eur. J. Mineral.* **3**, 751-768.
- \_\_\_\_\_, SOKOLOVA, E.V., KABALOV, YU.K., TEERTSTRA, D.K., KUNATH-FANDREI, G., GOETZ, S. & JÄGER, C. (1998): Intermediate scapolite: <sup>29</sup>Si MAS and <sup>27</sup>Al SATRAS NMR spectroscopy and Rietveld structure-refinement. *Can. Mineral.* **36**, 1267-1283.
- SKIBSTED, J., NIELSON, N. C., BILDSØE, H. & JAKOBSEN, H.J. (1991): Satellite transitions in MAS NMR spectra of quadrupolar nuclei. *J. Magn. Res.* **95**, 88-117.

- SOKOLOVA, E.V., GOBECHIYA, E.R., ZOLOTAREV, A.A. & KABALOV, YU.K. (2000) Rietveld structure-refinement of two marialites from the Kukurt deposit, Pamir. *Crystallogr. Rep.* (in press).
- \_\_\_\_\_, KABALOV, YU.K., SHERRIFF, B.L., TEERTSTRA, D.K., JENKINS, D.M., KUNATH-FANDREI, G., GOETZ, S. & JÄGER, C. (1996): Marialite: Rietveld structure-refinement and  $^{21}\text{Si}$  MAS and  $^{27}\text{Al}$  satellite transition NMR spectroscopy. *Can. Mineral.* **34**, 1039-1050.
- TEERTSTRA, D.K., SCHINDLER, M., SHERRIFF, B.L. & HAWTHORNE, F.C. (1999): Silvialite, a new sulfate-dominant member of the scapolite group with an Al-Si composition near the  $I4/m-P4_2/n$  phase transition. *Mineral. Mag.* **63**, 321-329.
- \_\_\_\_\_, & SHERRIFF, B.L. (1996): Scapolite cell-parameter trends along the solid-solution series. *Am. Mineral.* **81**, 169-180.
- \_\_\_\_\_, & \_\_\_\_\_ (1997): Substitutional mechanisms, compositional trends and the end-member formulae of scapolite. *Chem. Geol.* **136**, 233-260.
- TOSSELL, J.A. (1993): A theoretical study of the molecular basis of the Al avoidance rule and of the spectral characteristics of Al-O-Al linkages. *Am. Mineral.* **78**, 911-920.
- ULBRICH, H.H. (1973a): Crystallographic data and refractive indices of scapolites. *Am. Mineral.* **58**, 81-92.
- \_\_\_\_\_, (1973b): Structural refinement of the Monte Somma scapolite, a 93% meionite. *Schweiz. Mineral. Petrogr. Mitt.* **53**, 385-393.
- WÖLFEL, E.R. (1981): A new method for quantitative X-ray analysis of multiphase mixtures. *J. Appl. Crystallogr.* **14**, 291-296.
- \_\_\_\_\_, (1983): A novel curved position-sensitive proportional counter for X-ray diffractometry. *J. Appl. Crystallogr.* **16**, 341-348.
- ZOLOTAREV, A.A. (1993): Gem scapolites from the eastern Pamirs and some general constitutional features of scapolites. *Zap. Vser. Mineral. Obshchest.* **122**(2), 90-102 (in Russ.).

*Received November 26, 1999, revised manuscript accepted June 29, 2000.*